LBL-14331
Preprint c.2

Lawrence Berkeley Laboratory
UNIVERSITY OF CALIFORNIA

RECEIVED
LAWRENCE
BERKELEY LABORATORY

APR 17 1984

LIBRARY AND
DOCUMENTS SECTION

Submitted for publication

ANGULAR VELOCITY: A NEW DIMENSION IN NUCLEI

R.M. Diamond and F.S. Stephens

February 1984

TWO-WEEK LOAN COPY

This is a Library Circulating Copy which may be borrowed for two weeks. For a personal retention copy, call Tech. Info. Division, Ext. 6782.

NUCLEAR SCIENCE DIVISION

Prepared for the U.S. Department of Energy under Contract DE-AC03-76SF00098

LBL-14331 c.2

DISCLAIMER

This document was prepared as an account of work sponsored by the United States Government. While this document is believed to contain correct information, neither the United States Government nor any agency thereof, nor the Regents of the University of California, nor any of their employees, makes any warranty, express or implied, or assumes any legal responsibility for the accuracy, completeness, or usefulness of any information, apparatus, product, or process disclosed, or represents that its use would not infringe privately owned rights. Reference herein to any specific commercial product, process, or service by its trade name, trademark, manufacturer, or otherwise, does not necessarily constitute or imply its endorsement, recommendation, or favoring by the United States Government or any agency thereof, or the Regents of the University of California. The views and opinions of authors expressed herein do not necessarily state or reflect those of the United States Government or any agency thereof or the Regents of the University of California.

LBL-14331

Angular Velocity: A New Dimension in Nuclei

R.M. Diamond and F.S. Stephens

Nuclear Science Division
Lawrence Berkeley Laboratory
University of California
Berkeley, CA 94720

This work was supported by the Director, Office of Energy Research, Division of Nuclear Physics of the Office of High Energy and Nuclear Physics of the U.S. Department of Energy under Contract DE-AC03-76SF00098.

LBL-14331

Angular Velocity: A New Dimension in Nuclei

R.M. Diamond and F.S. Stephens

Nuclear Science Division
Lawrence Berkeley Laboratory
University of California
Berkeley, CA 94720

I. Introduction

Nuclear physics is a maturing science. Fifty years ago, with the discovery of the neutron, it was the forefront of our study of the ultimate constituents of matter and the arena in which two of the four known fundamental interactions were first encountered. It is still connected to this forefront; new forms of matter are sought at extremely high nuclear temperatures and densities, and attempts are being made to calculate nuclear properties from quantum chromodynamics, but such study has mainly separated off into elementary-particle physics. On the other hand, the nucleus is gradually being recognized as one of nature's most interesting quantal few-body systems. It concentrates into a single system many types of behavior, almost all of which are found individually in other systems. What is perhaps more interesting is that these types of behavior interact with one another in nuclei. A basic quantitative description of such interrelated phenomena is now developing. The main thrust of nuclear physics has thus become understanding in some detail this quantal few-body system and how it is related to other such systems.

There are many approaches to the study of nuclear physics. The classical method of Rutherford[1] is still one of the most important: shoot a projectile at the nucleus and see what happens. Rutherford analyzed the probability of scattering naturally occurring α-particles through various angles and deduced that the atom's positively charged nucleus was very small--~10,000 times smaller than the atom itself. Since that time nearly every conceivable projectile has been used: neutrinos, photons, electrons, mesons, nucleons, and nuclei themselves, ranging all the way from mass 2 (deuterium) to 238 (uranium). Depending on the projectile and bombarding energy, the result can be a very delicate transfer of a photon or nucleon, the complete fusion of target and projectile, or, at extremely high energies, an initial compression and heating of the target-projectile system followed by some kind of explosion. The analysis of "what happens" has produced much of our knowledge of nuclear structure. Another approach that started rather differently is the study of the de-excitation of nuclei excited by one means or another, originally by natural radioactive decay. Generally, these nuclei decay from state to state by emitting photons until the ground state is reached--much like atomic de-excitation--though this depends on the excitation energy and, to some extent, the nucleus, as we shall see. The result of such studies is a mapping of the lowest energy levels of a nucleus, which is also a major source of information about nuclear structure. Today, these methods are no longer distinct. The high-spin studies, for example, generally use a low-energy fusion reaction to bring large amounts of angular momentum into the fused system and then study the γ-ray decay of this system, which is usually completed in a nanosecond or so.

The information about nuclear structure that has been so far acquired is extensive and varied. Organizing it is inevitably somewhat subjective, but almost any scheme would have major divisions of "single-particle behavior" and "collective behavior", because the nucleus really is a "few-body" system (rather than a many-body system) and behaves accordingly. On the one hand, many nuclear properties can be determined largely by the motion of a single nucleon, and a shell model works well; the nucleons are assumed to move independently in their average potential, in close analogy to the atomic shell model. On the other hand, the nucleons, especially in heavier nuclei, often behave collectively, and there are close analogies to solid-state systems and to familiar macroscopic systems. This behavioral dichotomy is one of the fascinating aspects of nuclear structure and is the central theme of the high-spin studies we are interested in. Before embarking on a description of these studies, we will very briefly characterize these two aspects of nuclear behavior.

The independent-particle description of nuclei has a long history. The discovery of the neutron[2] in 1931 immediately triggered the nuclear shell model, which had previously been tried unsuccessfully with protons, electrons, and α-particles as constituents. It was proposed by Heisenberg[3] and some others who had just understood the structure of the atom, and, indeed, the similarities of these two systems are striking. The difference amounts mainly to replacing the long-range Coulomb potential of the atom with a short-range one more appropriate for the nucleus. There were initially serious doubts about an independent-particle model for nuclei, and it was quite some time before it was fully appreciated that the reason such a model works is that the

Pauli principle greatly restricts the possible scatterings, thereby increasing the mean free path. The next crucial idea was the large spin-orbit interaction ($\ell \cdot s$) in nuclei, which was proposed in 1949 by Mayer[4] and by Haxel, Jensen, and Seuss[5] and solved the problem that the early shell model had above mass 20. Because of the resulting large spin-orbit splitting, the highest-j orbitals drop down into the next lower shell and are called "intruders". They have different parity from their lower-shell neighbors, and thus they remain rather pure shell-model states and are easy to identify. These are the most important orbitals for building high angular momentum states. The (spherically symmetric) shell model implies that the nuclear levels are "bunched" into groups constituting the shells. A filled shell has extra stability, so that near closed shells nuclei tend to be spherical, or nearly so. On the other hand, between closed shells, spherical shapes are disfavored. The nucleus then explores the shape degree of freedom in order to find a lower energy. Closed shells can also occur for nonspherical shapes with high symmetry, resulting in extra stability for such shapes at these particular nucleon numbers. Such seemingly random variations in nuclear properties (like the shape) due to the detailed shell structure are called "shell effects".

One of the earliest collective phenomena observed in nuclei is fission, an evolution of nuclear shapes resulting in a division into two (or occasionally three) fragments. This process was discovered in 1939,[6,7] with profound consequences. Not long thereafter (1947) the first of the normal vibrational modes of the nucleus was discovered[8]—the so-called giant dipole resonance. This is an oscillation of neutrons against protons ("isovector"),

and only recently has it been joined by some "isoscalar" giant resonances--oscillations of the nuclear shape (protons and neutrons in phase). Yet a third collective effect, rotation, turns out to be most important for the present discussion. Not all nuclei can rotate, as we will see, but some of those that do have beautiful rotational level structures, similar to (though less perfect than) those of molecules. All three of these collective effects are very well described by the liquid-drop model introduced by Bohr and Kalckar[9] in 1937. This model considers the nucleus as a charged liquid drop, with volume, surface, Coulomb, and (later) rotational energies. Combined with "shell corrections", it gives the best existing estimates of the bulk nuclear properties. There is, however, at least one quantal collective effect in nuclei that is not described by the liquid-drop model, the pairing correlations. They are quite analogous to those in a superconductor or superfluid, and represent a coherent scattering of nucleon pairs among the levels near the Fermi surface. They play a role in high-spin studies, as we shall see. However, among these collective effects it is rotation that dominates the high-spin phenomena.

II. Making and Braking Large Angular Velocities

The amount of angular momentum a nucleus can hold is limited. The usual limitation has to do with fission, and it is easy to understand that the centrifugal force associated with rotation will tend to encourage this process. Without any barrier, fission is rapid—occurring in around 10^{-20} seconds. Thus to "exist" (i.e., longer than $\sim 10^{-20}$ seconds) the nucleus must have a barrier against fission. Such barriers can be estimated using the liquid-drop model,[10] and the angular momenta at which they just vanish are shown in Fig. 1 by curve ℓ_{II} as a function of nuclear mass (along the valley of beta stability). The maximum is about 100 $\hbar$ for A ~ 130. The curve falls off sharply at higher mass because of the increased Coulomb repulsion due to the additional protons. (Nuclei in the actinide region have measurable spontaneous fission lifetimes even at spin zero.) It falls off at lower mass because the nuclear moment of inertia (proportional to $A^{5/3}$) becomes smaller, so that for a given spin the rotational frequency is larger, thereby increasing the centrifugal force. If cold nuclei could be produced corresponding to the curve ℓ_{II}, spectroscopic studies might be possible up to this limit of angular momentum. But the heavy-ion fusion reactions that bring in this much angular momentum to the compound nucleus also bring in several tens of MeV of excitation energy, greatly increasing the fission probability. To prevent fission, another process must successfully compete to de-excite the nucleus, and at such excitation energies this can only be particle evaporation. The time scale for this particle evaporation is 10^{-17}-10^{-18} s, and in order to slow the fission down to such times, a fission barrier of the order of the neutron binding energy (~8 MeV) is required. The dashed line in Fig. 1 corresponds to an 8-MeV fission barrier, below which particle evaporation should dominate.

There is another interesting aspect shown in Fig. 1. The curve ℓ_{II} is determined by two different types of nuclear shape in different mass regions. At the highest masses the shape where the fission barrier just vanishes is spheroidal, more specifically, oblate. In fact, this is the stable shape everywhere below the curve ℓ_I. In the region between ℓ_I and ℓ_{II} the equilibrium shape is ellipsoidal, generally triaxial, and elongates with increasing spin. These shapes are well known in the general context of equilibrium shapes of rotating objects. If one just reverses the sign of the Coulomb energy term in the liquid-drop model, the equations describe a rotating gravitational object with surface tension (i.e., a liquid). To have a surface energy comparable to its gravitational energy (a nucleus has Coulomb and surface energies comparable), the object would have to be of order 10 meters in diameter (density taken as 5, surface tension like water). A rotational period of about an hour would bring the object to the shape boundary analogous to the line ℓ_I in Fig. 1. If asteroids go through molten stages, they would be an example of such a system. The limit of negligible surface tension was applied to calculations of the shape of astronomical bodies (first the earth) by Maclaurin[11] in 1742. The spheroidal shapes below ℓ_I in Fig. 1 bear his name, whereas the ellipsoidal ones above were found about a hundred years later by Jacobi.[12] If, on the other hand, one increases the surface energy greatly relative to the gravitational energy, one describes weightless rotating droplets (as were examined by the Apollo astronauts using blobs of water). One can even consider negative masses (moments of inertia) and describe bubbles in ordinary fluids (or nuclei, for that matter). It is apparent that the nuclear properties depicted in Fig. 1 are related to a very widespread type of behavior. Since the dashed line in Fig. 1 includes some area above ℓ_I, there is a hope to find some of these

elongated shapes in nuclei at very high spins. They go under the name "superdeformed nuclei" and will be energetically favored by shell effects for some nuclei and disfavored for others. There is, at present, a great interest in identifying such shapes, as they would give interesting information about the applicability of the liquid drop model at the very highest spins.

A schematic illustration of the decay modes for a nucleus of mass ~160 is shown in the "phase-like diagram" of Fig. 2. The coordinates are nuclear excitation, E*, and spin, I. The heavy lines divide the E*-I space into regions of different decay modes. The yrast line is the locus of states of lowest energy for a given spin, so that no states exist in the nucleus below this line. A typical heavy-ion fusion reaction might lead to an initial excitation energy of ~65 MeV and a spin distribution ranging from 0 to ~65 $\hbar$ as indicated by the light line in Fig. 2. As long as the nucleus has sufficient energy above the yrast line to emit nucleons (~10 MeV), it usually does so; γ-ray emission is too slow to compete well with particle evaporation. But at excitations below the nucleon binding energy, γ-ray emission takes over and de-excites the nucleus to its ground state. The angular momentum removed by the particle evaporation is small if neutrons or protons are involved (~1 $\hbar$ per particle and only a few particles). In Fig. 2 it can be seen that the highest spins (longest γ-ray cascades) will be associated with the fewest neutrons emitted. It is now known that these γ-ray cascades have two principal types of transitions. The "statistical" transitions carry off energy but little angular momentum and so cool the nucleus towards the yrast line. The "yrast-like" transitions follow paths roughly parallel to the yrast line and remove the angular momentum of the system. These latter are sometimes collective rotational transitions, and sometimes not. There are an enormous number of pathways from the beginnings

of a high-spin γ cascade until a region near the yrast line is reached, with the result that no single transition has enough intensity to stand up in the spectrum (with present techniques). This is the origin of the name "continuum" γ-ray spectrum, though this is not a true continuum. When the nucleus has cooled sufficiently the population condenses into a few pathways and the transitions in these pathways stand up in the spectrum and are resolved. This typically happens in the spin range 30-40 $\hbar$ for masses around 160, and it provides a logical division in high-spin studies. In the lower-spin region, one can employ all the techniques of conventional γ-ray spectroscopy and develop detailed information on the nature of the transitions and states involved, as discussed in Section IV. At the higher spins where the population is spread out too much to permit the study of individual transitions, new techniques are providing a picture of the average nuclear behavior. These are described in Section V. There is, of course, a large effort underway to resolve this "continuum" spectrum using new detector systems, and the prospects here comprise much of Section VI.

III. Shape Effects

One of the most important factors in determining the physics of high-spin states is simply the rotational behavior of rigid classical objects. In Fig. 3 the moment of inertia of such an object (solid lines) is compared with that of a rigid sphere for a variety of shapes and rotational axes. The shape and axis is defined by γ, which varies from -120° to 60° as the object varies from a prolate shape rotating about its symmetry axis, through oblate and prolate shapes rotating about axes perpendicular to the symmetry axis, to an oblate shape rotating about its symmetry axis. These axially symmetric shapes are shown by small drawings in Fig. 3, and the regions between correspond to shapes with all three axes different—triaxial. The deformation is given in terms of a quantity ε, which is to lowest order just $\Delta R/R$, the difference in radii divided by the average radius. Values of ε around 0.3 are typical for the familiar deformed rare-earth and actinide nuclei, and 0.6 corresponds to an axis ratio of 2:1, the largest known in nuclei. The largest moments of inertia, and therefore the lowest rotational energies, occur for the range of shapes between $\gamma = 0^\circ$ and 60°. The very largest moment of inertia for moderate deformations is for $\gamma = 60^\circ$, an oblate shape rotating around its symmetry axis, and it is for this reason the earth has such a shape. The full liquid-drop model (LDM) treatment of a rotating nucleus[10] including surface and Coulomb energies in addition to these geometrical shape considerations is shown by the dots in Fig. 3. It is apparent that there is no strong shape preference in these additional LDM terms, so that simple geometry determines the liquid-drop shapes. This is important, since the LDM is our best guide to such macroscopic nuclear properties and is even the average limit to which some of the microscopic (individual particle) models are normalized.

In order to see how significant these geometrical shape effects are, one must choose a mass and spin, and for A = 160 and I = 60, an energy scale is given on the right side of Fig. 3. The variation for $\varepsilon = 0.3$ of about 10 MeV is larger than typical shell effects (~3 MeV) so that for this spin the shape effects considered here should be dominant. However, the rotational energy varies as I^2 so that, for I = 30, the shell effects and these classical shape effects should be about equivalent, and below I ~ 20 the shell effects will dominate. The arguments made here would seem to apply only for collective nuclear rotations, and even then only if the nuclear moment of inertia has the rigid-body value, neither of which is obviously the case. In fact, however, most people do believe that rotating nuclei at high spins will, on average, have the rigid-body moment of inertia, and this has been shown to be the case for independent particle motion in a rotating anisotropic harmonic-oscillator potential.[13] (The smaller moments of inertia observed at low spins are due largely to the pairing correlations, which should be quenched by the Coriolis force above ~30 $\hbar$, as will be described.) Furthermore, even in noncollective cases, it has been shown (for a Fermi gas) that the trajectory of lowest levels follows that given by rotating the appropriately shaped rigid body.[14] Thus, these geometrical arguments are expected to be valid, and shapes in the $\gamma = 0\text{–}60^\circ$ range should dominate at high spin, i.e., above ~30 $\hbar$ in the A = 160 region. There are a number of detailed microscopic calculations that agree with these expectations.

There is a further aspect of these shapes that is important. The rotation of a nucleus about an axis perpendicular to the symmetry axis is a collective rotation with smooth bands--$E(I) \propto I(I + 1)$--and strongly enhanced E2 transitions connecting the levels. There are many beautiful examples of such rotors in the region around mass 160, one of which is shown in the left part of Fig.4. This is the lowest-lying sequence of levels in ^{158}Er.

The odd spins are missing, indicating that the two ends of the nucleus are indistinguishable (symmetry under rotation of 180° about the x or y axis--like homonuclear diatomic molecules). Also the electric quadrupole transitions connecting the levels generally vary smoothly in energy and are enhanced by about 150 times over that expected for a single proton, indicating a collective quadrupole shape as schematically shown on the far left of Fig. 4. On the other hand a quantal system like the nucleus cannot rotate around a symmetry axis. This degree of freedom is contained in the single-particle motions. Thus a nucleus with $\gamma = 60°$ builds up its angular momentum by aligning that of one or more individual nucleons with the symmetry axis, like spherical closed-shell nuclei. An example of this behavior is shown on the right side of Fig. 4. The ^{147}Gd nucleus is nearly spherical in its ground state and builds its angular momentum by aligning particles as schematically illustrated at the far right of Fig. 4. The aligned particles give the system an oblate shape that "effectively rotates about its symmetry axis"--$\gamma = 60°$. The motion is almost completely noncollective and the transitions in the ^{147}Gd scheme are quite irregular in energy and are not enhanced. Most nuclei combine these types of behavior, leading to triaxial shapes between 0° and 60°. This tendency can already be seen in the ^{158}Er scheme, where there are irregularities around spins 16 and 26, which correspond to single-particle alignments. Our understanding of this alignment process was a major step for high-spin studies in the last decade and is described in the next section.

IV. Rotational Alignment

The lack of smoothness in rotational spectra came as a surprise in 1971 when a discontinuity was found in the energies of the ground-state rotatonal bands of several rare-earth nuclei.[17] As the nucleus de-excites from a high initial spin, the regular increase in rotational period (slowing down) is interrupted occasionally by rather sizeable decreases. These correspond to internal rearrangements, "nuclearquakes", and are generally called "backbends". It is amusing to compare them with another type of quake—"starquakes". Neutron stars or "pulsars" are also rapidly rotating systems that are slowing down. Occasionally they too have sudden internal rearrangements that decrease the moment of inertia and therefore speed up the rotation (called "glitches"). An earthquake is a similar phenomenon, but the change in the earth's rotation from even the largest earthquake is much too small to measure. It is quite common that rapidly rotating objects modify their internal structure to produce larger moments of inertia, and these modifications revert back, often in sudden jumps, as the system slows down. The interesting question for each system has to do with the nature of the internal modification. The slowing down of the nucleus ^{158}Er below spin 20 is compared with the pulsar Vela in Fig. 5. The behaviors are quite similar, though the percentage change in the nuclear case is much larger. The pulsar glitches are not too well understood at present—early explanations had to do with a sudden breaking of the solid crust on the neutron star, but more recent ones involve vortices in the flow pattern. The nuclear glitch is much better understood and is related to the pairing correlations in nuclei.

The nuclear pairing correlations play an important role up to spins around 30 $\hbar$. The nucleon orbitals in a static deformed potential are twofold degenerate, corresponding to a time reversal of their motion. This situation for an axially symmetric prolate nucleus is illustrated at the top of Fig. 6. The angular momentum, j, of the nucleon has projections, $\pm\Omega$, along the symmetry axis and, when occupied by two nucleons, results in total angular momentum zero. Every orbital, characterized by j,Ω can give rise to such a spin-zero pair. The nucleons in a filled orbital near the Fermi level can scatter as a pair into a nearby empty orbital, and the coherent scattering pattern that develops comprises the nuclear pairing correlations. It is interesting that these correlations are closely analogous to those in superconductors or superfluids. In fact, the equations of Bardeen, Cooper, and Schreifer[18] (BCS) that first gave an explanation of superconductivity are taken over exactly into the nuclear case[19-21] and give nearly correctly both the systematic mass difference between even-even nuclei (all paired, zero quasiparticles) and odd-mass nuclei (one quasiparticle) and the ~2 MeV level gap in even-even nuclei (zero to two quasiparticle energy).

These pairing correlations affect the ability of the nucleus to generate angular momentum. It is easy to see that this is plausible since, insofar as the pairs are coupled to spin zero, they can contribute nothing toward generating angular momentum. This causes a factor of two or three reduction in the nuclear moment of inertia, which is given reasonably well by the BCS wave functions. It follows that angular momentum will tend to weaken the pairing correlations, thus increasing the moment of inertia and reducing the rotational energy. The mechanism of this weakening is the Coriolis force, which acts oppositely on the two members of the pair, lifting their degeneracy. Ultimately the Coriolis force wants to align the particle angular

momentum as well as possible with the rotation axis, as illustrated at the bottom of Fig. 6. This process is analogous to the effect of a magnetic field on the paired electrons in a superconductor, where there is a sudden change back to the normal state when a critical magnetic field is reached. There were initial thoughts that a nucleus might behave similarly when a critical angular momentum is reached, but the nucleus differs from the superconductor in at least two respects: 1) rather than approximately Avogadro's number of electrons, there are ~100 nucleons in the nucleus, of which only 10-20% are near the Fermi level and thus participating in the pairing correlations, and 2) the nucleons have a wide spread of j values ranging from 1/2 to ~13/2 (for mass around 100). The result is that the nuclear phase transition is not sharp but broad--i.e. gradual--as evidenced by a gradual rise in the moment of inertia for spins up to ~20-30 $\hbar$. But, within this gradual rise is occasionally a large irregularity that corresponds to the rather complete alignment of a particular pair of high-j nucleons. This comes about because the Coriolis force is proportional to j and thus affects high-j particles most strongly, so that at some point the nucleus finds it energetically most favorable to align such a pair rather completely while keeping the pairing correlations among the lower-j nucleons. This is what causes the nuclear quakes shown in Fig. 5. In ^{158}Er and many other nuclei of that region, it is the sudden alignment of a pair of $i_{13/2}$ (ℓ = 6, s = +1/2) neutrons[22] that causes the large irregularity at frequencies around 0.25 MeV (I ~ 16). Some of these same nuclei suffer a second smaller discontinuity when a pair of $h_{11/2}$ protons aligns at frequencies around 0.4 MeV (I ~ 26). Such detailed information is not available at frequencies much higher than this, for reasons that will become apparent in the next section. However, this rotation alignment of high-j nucleons gives much more information about nuclear structure than might be apparent from the discussion so far.

There is a point of view developing that angular velocity or frequency is an important dimension along which nuclear properties can be measured. In this picture a rotational band is just a sequence of snapshots of the same configuration at increasing rotational frequencies, and there are a number of properties that can be readily observed in these snapshots. The alignments discussed above stand out in the various bands like mileposts, and the present discussion will be limited to these mileposts and, further, to just the critical frequency, $\hbar\omega_c$, at which they occur. Much of the information so far available is on the alignment of two $i_{13/2}$ neutrons in nuclei around mass 160. In Fig. 7 the aligned angular momentum, i, for this pair (measured by the difference in angular momentum between the band under consideration and a reference band) is plotted against rotational frequency (approximately half the rotational γ-ray energy) for three bands. The solid line is for the lowest-energy band in the even-even nucleus ^{162}Yb, which is much the same as the band in ^{158}Er plotted in Fig. 4. The critical frequency is about 0.26 MeV and the aligned angular momentum is ~10 $\hbar$ (12 $\hbar$ is the maximum for two $i_{13/2}$ neutrons). There are methods to evaluate both these quantities more accurately, but that is not necessary here. The dashed lines are for two bands in the nucleus ^{163}Yb with one additional neutron located in an orbital labeled either E or F. These orbitals comprise a time-reversed pair at zero rotational frequency and are not very pure shell-model states, though their dominant component is $h_{9/2}$. In the even-even nucleus ^{162}Yb, this pair of states (E,F) is available for the pairing correlations, and, in particular, a pair of $i_{13/2}$ neutrons can scatter into it. On the other hand, in ^{163}Yb it is blocked by the odd nucleon for the bands based on either E or F. The pairing correlations are thereby weaker--in general and in particular for a pair of $i_{13/2}$ neutrons. It is then easier to unpair and align the $i_{13/2}$

neutrons, and this occurs at a lower rotational frequency, ~0.22 MeV, as seen in Fig. 7. The shift is clear and closely reproducible in other nearby nuclei.[24] This shift can be related through calculations to the change in the pairing correlations involved and turns out to correspond to a 20-30 reduction in pairing. The calculation of such properties is done by cranking a deformed shell-model potential around an axis perpendicular to the symmetry axis and can relate this frequency shift, $\delta\hbar\omega_c$, to a change in the pairing gap, $\delta\Delta$, with reasonable confidence. Thus we learn that blocking just one orbital near the Fermi level reduces the pairing correlations appreciably, a result that is confirmed by other kinds of experiments--transfers of pairs of nucleons and directly from the odd-even mass difference. The pairing correlations in nuclei are marginal, and three or four blocked levels of either type (protons or neutrons) are enough to destroy the correlations for that nucleon type. But the analysis of data like that shown in Fig. 7 can be carried considerably further.

The discussion so far has involved blocking one particular pair of orbitals, E and F. Others can be blocked, and to date most of the calculations of nuclear pairing effects assume identical results for blocking any orbital equally distant from the Fermi level (called "monopole pairing" for reasons that will become apparent). This is, in fact, not very reasonable, since the aligning neutrons in this case are $i_{13/2}$ (with a specific orientation, implied by their alignment) and some orbitals will have better spatial overlap with these than others. It seems likely that the more similar ones will affect the pairing more (larger $\delta\hbar\omega_c$), but no experimental information previously existed on such detailed properties. One measure of the shape of an orbit is its quadrupole moment relative to the nuclear symmetry axis (this is the lowest order useful moment since nucleon

electric dipole moments vanish due to parity conservation). Figure 8 is a plot of the shift in the alignment frequency for two $i_{13/2}$ neutrons, $\delta\hbar\omega_c$, vs the quadrupole moment of the blocked orbital.[25] The aligning neutrons have a large positive (prolate) quadrupole moment ($\sim$+4 fm^2), and the magnitude of $\delta\hbar\omega_c$ is reasonably clearly correlated with the similarity of the quadrupole moment of the blocked state to this value. In fact, the $h_{11/2}$ ($11/2^-$ [505]) orbital is strongly oblate (very different), and blocking it produces no difference in the pairing behavior of the $i_{13/2}$ neutrons ($\delta\hbar\omega_c \sim 0$). Such higher order effects are referred to as "quadrupole pairing". Their appearance results from the few-body nature of the nucleus, and gives us some information about pairing phenomena which do not occur in macroscopic systems such as superconductors.

Exploitation of the rotational-frequency dimension has just begun. Studies of the type outlined above can be extended to 1) additional blocked orbitals and 2) other aligning pairs. Also, it is apparent in Fig. 7 that the amount of aligned angular momentum, i, varies between the even (0-2 quasiparticle) and the odd (1-3 quasiparticle) systems. This is probably also a pairing effect but is not yet so well understood as the "critical-frequency" effects discussed above. There are still other properties to study as a function of frequency. The fact that E and F are split by the rotation is due to their different symmetry properties. Such "signature splitting" appears to be sensitive to details of the shape and may thus give us more insight into the shapes of nuclei and how they change with frequency (and other properties). In addition, the process of quenching the pairing correlations by the presence of several quasiparticles (blocking) and a high rotational frequency (Coriolis effects) is under rather intensive study at this time.

Thus far it has not been possible to obtain quantitative measures of this quenching, though it is clearly rather large in some cases. This "new spectroscopy" is just beginning and seems likely to be quite exciting. It is in addition to the very interesting question of what happens to the nucleus at still higher frequencies, which will be taken up in the next section.

V. The Highest Spins

Above about 30 or 40 $\hbar$, individual transitions cannot at present be resolved following heavy-ion fusion reactions. The reason for this is not fundamental, but simply that too many de-excitation pathways exist, as was discussed in Section II. Thus, to study higher spins we must study unresolved γ-ray spectra. Most of the techniques so far devised to do this involve measuring average moments of inertia, and considerable progress has been made.

As a consequence of the interplay between collective and single-particle motions, there are a variety of moments of inertia one can measure and compare with detailed nuclear model calculations. The first distinction to make is between kinematic and dynamic values. The equation for the rotational energies of a symmetrical top is:

$$E(I) = \frac{\hbar^2}{2\mathcal{J}} I(I + 1) \quad , \tag{1}$$

where $\mathcal{J}$ is the moment of inertia. One sees that a moment of inertia may be defined from the first derivative of the energy with respect to spin:

$$\frac{\mathcal{J}^{(1)}}{\hbar^2} = I\left(\frac{dE}{dI}\right)^{-1} = \frac{I}{\hbar\omega} \quad , \tag{2}$$

where $\mathcal{J}^{(1)}$ is called the "kinematic" moment of inertia because it has to do with the motion of the system--the ratio of angular momentum to angular frequency. It is also apparent that the second derivative leads to a definition:

$$\frac{\mathcal{J}^{(2)}}{\hbar^2} = \left(\frac{d^2E}{dI^2}\right)^{-1} = \frac{dI}{\hbar d\omega} \quad , \tag{3}$$

where $\mathcal{J}^{(2)}$ is called the "dynamic" moment of inertia because it has to do with the way the system will respond to a force. If there is only the kinetic energy term as given in Eq. 1, these are equal; but, in general, when there

are additional I-dependent terms in the Hamiltonian these two moments of inertia will differ. In the present case, the Coriolis force perturbs the internal nuclear structure, giving rise, in lowest order, to an $(I \cdot j)$ term, so that $\mathcal{J}^{(1)} \neq \mathcal{J}^{(2)}$. This situation is not uncommon in other branches of physics. The arguments carry over into translational motion, where $p^2/2m$ is analogous to $I^2/2\mathcal{J}$, and additional momentum-dependent terms in the Hamiltonian give rise to two observed masses. An electron moving in a crystal lattice is a close analog,[26] where the kinematic mass determines the level density and related statistical mechanical properties; whereas the response of the electron to an external force depends on a different, dynamic mass. In cases where the extra (angular) momentum-dependent term(s) depend on (I^2) p^2 (or so long as they can be expanded in lowest order as such) they can be taken together with the kinetic term to give a renormalized (moment of inertia) mass.

These two moments of inertia can be defined in principle for any sequence of states desired, but certain ones occur rather naturally in the decay processes. If the particle configuration is frozen, so that one is confined to a collective rotational band, the appropriate moments of inertia are $\mathcal{J}^{(1)}_{\text{band}}$ and $\mathcal{J}^{(2)}_{\text{band}}$. When there is no perturbation (alignment, shape change, etc.) of the internal structure along this band, these correspond to the true "collective" values, and this is an approximation often made. In general, however, a single decay pathway involves a sequence of bands having different alignments or shapes. It is then natural to define "effective" moments of inertia $\mathcal{J}^{(1)}_{\text{eff}}$ and $\mathcal{J}^{(2)}_{\text{eff}}$, which include <u>both</u> the collective contribution <u>and</u>, in addition, contributions caused by changes in particle alignment and shape.

For the unresolved spectra from the highest spin states, the population is spread over many bands in many decay sequences. Nevertheless, average values for these moments of inertia can be determined in the following ways.

The γ-ray spectrum from a rotational nucleus is highly correlated in time, spatial distribution, and energy. For a perfect rotor, this spectrum is composed of equally spaced lines, up to some maximum energy corresponding to the decay of the state with highest angular momentum. One aspect of this distribution is that no two γ rays have the same energy. If plotted on a two-dimensional diagram of $E_\gamma^{(1)}$ vs $E_\gamma^{(2)}$, such energies give a pattern with no points along the diagonal and a series of ridges parallel to it. The width of the "valley" along the diagonal is determined by the difference between rotational γ-ray energies and thus gives values for $\mathcal{J}^{(2)}_{band}$. The important point is that the spectrum need not be resolved to determine the valley width. All that is required is that the populated bands have somewhat similar moments of inertia at a given frequency (γ-ray energy).

The data in Fig. 9 come mainly from ^{159,160}Er nuclei formed by bombarding ^{124}Sn with ^{40}Ar at sufficient energy (185 MeV) to bring into the fused system all the angular momentum the nucleus can hold (~70$\hbar$). The data have been "symmetrized" around the diagonal in order to improve the statistics and have an "uncorrelated" background subtracted. A valley is clear up to energies ~1 MeV, and again probably from 1.1 to 1.2 MeV. Resolved lines have been seen in this case only up to ~0.8 MeV. The width of the valley in both the upper and lower region is about the same and can be evaluated to give $\mathcal{J}^{(2)}_{band}/\hbar^2 \approx 50$ MeV^{-1}, around two-thirds of the rigid-body value. Together with the effective moments of inertia, this is an important clue as to the nuclear structure in this region, as will be seen.

There are other important features in these correlation plots. For example, the valley is sometimes filled by irregularities in the bands, such as alignments. These produce several transitions in the same energy region, and not only fill the valley but produce "stripes" of higher coincidence intensity at these γ-ray energies. The analysis of these features is not yet very far advanced. There are also two or three recent cases[28-30] where the $\mathcal{J}^2_{band}$ values measured in this way are very constant and near the full rigid-body value. This is a puzzle, as it seems to leave no room for alignment effects which are expected, as discussed below. There is clearly more information in these correlation plots than is at present understood.

The effective moments of inertia are simpler in some respects. They involve only relating a collective γ-ray energy with a spin or measuring the number of γ rays in an energy interval. The former gives $\mathcal{J}^{(1)}_{eff}$ values and has been measured several different ways, originally by relating the maximum γ-ray energy in a spectrum with the estimated maximum spin input.[31] However, $\mathcal{J}^{(2)}_{eff}$ is much more sensitive to the nuclear structure. It is possible to measure $\mathcal{J}^{(2)}_{eff}$ because, in a spectrum consisting only of "stretched" electric quadrupole ($I \rightarrow I-2$) transitions (which is known to be a good approximation in regions of rotational behavior), the number of transitions in a given γ-ray energy interval is just half the spin removed by that interval. If one knows the fraction of the observed population that goes through the interval, then the height of the spectrum gives directly $\mathcal{J}^{(2)}_{eff}(\omega)$. This had been recognized earlier, but the difficulty was to find the feeding as a function of spin. Recently a method was developed[32] using the spectra from two similar but slightly shifted spin distributions, whose difference is generally proportional to the feeding curve.

Figure 10(top) shows a spectrum due mainly to ^{160}Er decaying from a rather broad distribution of spin centered at ~55ħ. The spectrum of statistical γ rays, whose high-energy tail is seen above ~2 MeV, is subtracted leaving essentially pure collective transitions, and the $\mathcal{J}^{(2)}_{eff}$ values shown by the solid line in Fig. 10(bottom) result from correcting this for feeding. Two other cases, ^{162}Yb and ^{166}Yb, are also shown in Fig. 10(bottom). The general rise at low frequencies in all these nuclei is due to the quenching of the pairing correlations, and the irregularities below $\omega \approx 0.3$ MeV result from partially resolved individual γ-ray transitions and the known alignments (backbends), which cause several transitions to pile up at the same frequency. The band moments of inertia from the correlation data are plotted as lighter lines in the regions where they have been determined. The rise in the effective moments of inertia above frequencies of 0.5 MeV seem to be associated with a drop in the band values. This suggests that alignments are becoming more important contributors of angular momentum. The higher values for the Yb (Z = 72) nuclei compared with ^{160}Er (Z = 70) suggest that protons play an important role here, which is in accord with calculations that predict proton $h_{9/2}$ and $i_{13/2}$ alignments in this frequency region.

While such data do not give the detail obtained at lower spins from studies of resolved lines, they are, nevertheless, beginning to give important insights into the physics of these highest spin states. No doubt techniques to study unresolved spectra will be developed considerably further if we do not learn how to resolve this continuum spectrum.

VI. The Future

The study of nuclei at high spin is an active area right now. There are new types of detector systems coming into operation and a rapid development of the theoretical tools to interpret the data and to serve as a guide in further data acquisition. It seems appropriate to conclude with a brief outline of the prospects in this field.

The information on high-spin states comes mostly from studies of γ rays; thus there is a strong incentive to develop more powerful γ-ray detector systems. An obvious goal is to measure the energy and angle of every γ ray emitted from a decaying high-spin state (up to 35 transitions in some cases). Two 4π detector systems have been built to accomplish this. These instruments are both shells of NaI about eight inches in inner radius and seven inches thick (insuring almost complete absorption of all γ rays). To isolate the individual γ ray, the shell is divided into many elements, 72 for the system built at Oak Ridge[33] and 162 for the one in Heidelberg.[34] A photograph of the Oak Ridge system is shown in Fig. 11. These instruments can measure the number of γ rays and the total γ-ray energy emitted, each with about 20% resolution (full width at half-maximum). In general, for the decay of high-spin states the number of γ rays is related to the initial spin and the total energy to the initial excitation energy. Thus these instruments can isolate a rather small initial population region as can be visualized in Fig. 2. The spectrum of γ rays from this limited region should be much simpler to study than that from the entire reaction, perhaps even fully resolvable. Furthermore, the region can be moved in spin or excitation energy (nuclear temperature) by changes in the gating conditions. Such possibilities are exciting and, already, out of some initial studies,[35] evidence for a dependence of the γ-ray spectrum on initial temperature has been found.

These "crystal balls" also measure the energy and angle of (nearly) every γ ray. This will surely be interesting to explore but is not quite so powerful as it might be because the γ-ray energy resolution in NaI is rather poor--5-6% (full width at half-maximum) for a 1 MeV γ ray. In fact, these crystal balls will probably often be used in conjunction with detectors of higher energy resolution, mainly germanium semiconductor detectors, which give about 0.2% resolution at 1 MeV (but cannot be made so large). Such considerations have led to "combination" detector systems--a low-resolution highly efficient shell to give the initial-state selection (as described above) coupled with an array of high-resolution Ge detectors. One such apparatus exists at Daresbury.[36] A sketch of such a system being constructed at Berkeley[37] is shown in Fig. 12. The inner shell here is made of 44 bismuth germanate elements—a scintillator with worse energy resolution than NaI but 2-3 times more compact (higher density and higher effective atomic number). It can serve to define the initial state nearly as well as the NaI balls and allows ~20 germanium detectors within 15 cm of the target. Each germanium detector is surrounded by a cylindrical shell of a scintillator (also bismuth germanate, in this case), which detects photons (Compton) scattered out of the germanium (leaving a partial energy in the germanium) and thus permits such events to be rejected. This improves the response function of the germanium detector by a factor of about three, from ~20% full-energy events for a 1 MeV γ to ~60%. This detector system is aimed at acquiring high rates not only of double coincidences but of triple and even quadruple coincidences. Coupled with the high resolution of the germanium detectors,

this will specify a decay sequence more precisely than by any other present technique, i.e., give very high "effective" resolving power. Such systems will contribute both toward resolving the continuum and to the detailed spectroscopy of the lower spin regions.

The high-spin field is thus giving rise to a new generation of data acquisition systems. Fortunately, the theoretical developments have kept pace. Single-particle motion can be calculated in deformed potentials of several types, and, further, these can be cranked about various axes to simulate the rotation. Such calculations, though still approximate, can be an excellent guide. Virtually all the properties now measured can also be calculated, and comparison provides a stimulus both to interpreting the experimental data and to improving the calculations. In the lower spin regions the pairing-correlation studies discussed in Section IV are an example of this process.

There are many open questions to address. Two in the lower spin region are (1) where and how are the pairing correlations finally quenched by the rotation, and (2) what is the detailed nuclear shape and how does it vary for different bands (configurations), as a function of spin in a single band, and as a function of nuclear temperature. At higher spins the questions are broader. What are the appropriate quantum numbers to describe the system? This is related to the question of whether there are still large single-particle effects (irregularities) or whether the nucleus has been homogenized at the highest spins and the motion has become fully collective. One is examining in detail here the generation of collective properties out of an underlying single-particle structure. Then there are the interesting

questions connected with "superdeformations" and the shape evolution connected with fission. Over a broad range of masses the angular momentum we can study is limited mainly by fission, so it is clear we can reach situations where the centrifugal force produces major changes. How these are influenced by shell effects or other aspects of the single-particle motion will be fascinating to study. The nucleus provides a chance to study a few-body quantal system over a broad range of a variable, the rotational frequency. The results will surely enrich our perspectives on such systems.

This work was supported by the Director, Office of Energy Research, Division of Nuclear Physics of the Office of High Energy and Nuclear Physics of the U.S. Department of Energy under Contract DE-AC03-76SF00098.

References

1. E. Rutherford, Phil. Mag. 21, 669 (1911)

2. J. Chadwick, Proc. Roy. Soc. A136, 692 (1932)

3. W. Heisenberg, Z. Phys. 77, 1 (1932)

4. M. G. Mayer, Phys. Rev. 75, 1969 (1949)

5. O. Haxel, J. H. D. Jensen, and H. E. Suess, Phys. Rev. 75, 1766 (1949)

6. O. Hahn and F. Strassman, Naturwiss. 27, 11 (1939)

7. L. Meitner and O. R. Frisch, Nature 143, 239 (1939)

8. J. C. Baldwin and G. S. Klaiber, Phys. Rev. 71, 3 (1947)

9. N. Bohr and F. Kalckar, Kgl. Danske Videnskab. Selskab, Mat-fys. Medd. 14, 10 (1937)

10. S. Cohen, F. Plasil, and W. J. Swiatecki, Ann. Phys. 82, 557 (1974)

11. C. Maclaurin, A Treatise on Fluxions (1742)

12. C. G. J. Jacobi, Uber die Figur des Gleichgewichts, Poggendorff Annalen der Physik und Chemie 33, 229 (1834)

13. A. Bohr and B. R. Mottelson, Mat. Fys. Medd. Dan. Vid. Selsk., 30, no. 2 (1955)

14. A. Bohr and B. R. Mottelson, Nuclear Structure, vol. 2, p. 80 (W. A. Benjamin, Inc., Reading, Mass.) 1975

15. J. Burde, E. L. Dines, S. Shih, R. M. Diamond, J. E. Draper, K. H. Lindenberger, C. Schuck and F. S. Stephens, Phys. Rev. Lett. 48 530 (1982)

16. P. Kleinheinz, R. Broda, P. J. Daly, S. Lunardi, M. Ogawa, and J. Blomqvist, Z. Phys. A290, 279 (1979); P. Chowdhury, H. Emling, D. Frekers, R. V. F. Janssens, T. L. Khoo, S. Bjørnholm, J. Borggreen, J. Pedersen, G. Sletten, Y. H. Chung, M. Kortelahti, Workshop on Nuclear Structure at High Spin, Risø, May, 1983

17. A. Johnson, H. Ryde, and J. Sztarkier, Phys. Lett. 34B, 605 (1971)

18. J. Bardeen, L. N. Cooper, and J. R. Schrieffer, Phys. Rev. 106, 162 (1957); 108, 1175 (1957)

19. A. Bohr, B. R. Mottelson, and D. Pines, Phys. Rev. 110, 936 (1958)

20. S. T. Belyaev, Mat. Fys. Medd. Dan. Vid. Selsk. 31, no. 11 (1959)

21. A. B. Midgal, Nucl. Phys. 13, 655 (1959)

22. F. S. Stephens and R. S. Simon, Nucl. Phys. A183, 257 (1972)

23. B. Herskind, private communication (1982)

24. J. D. Garrett, O. Andersen, J. J. Gaardhøje, G. B. Hagemann, B. Herskind, J. Kownacki, J. C. Lisle, L. L. Riedinger, W. Walus, N. Roy, S. Jönsson, H. Ryde, M. Guttormsen, and P. O. Tjøm, Phys. Rev. Lett. 47, 75 (1981)

25. J. D. Garrett, G. B. Hagemann, and B. Herskind, Nucl. Phys. A400, 113c (1983)

26. A. Bohr and B. R. Mottelson, Phys. Scr. 24, 71 (1981)

27. M. A. Deleplanque, F. S. Stephens, O. Andersen, C. Ellegaard, J. D. Garrett, B. Herskind, D. Fossan, M. Neiman, C. Roulet, D. C. Hillis, H. Kluge, R. M. Diamond, and R. S. Simon, Phys. Rev. Lett. 45, 172 (1980)

28. H. G. Price, C. J. Lister, B. J. Varley, W. Gelletly, and J. W. Olness, Phys. Rev. Lett. 51, 1842 (1983)

29. C. Schuck, N. Bendjaballah, R. M. Diamond. Y. Ellis-Akovali, K. H. Lindenberger, J. O. Newton, and F. S. Stephens, (to be published)

30. R. Chapman, J. C. Lisle, J. N. Mo, E. Paul, A. Simcock, J. C. Willmott, J. R. Leslie, H. G. Price, P. M. Walker, J. C. Bacelar, J. D. Garrett, G. B. Hagemann, B. Herskind, A. Holm and P. J. Nolan, Phys. Rev. Lett. 51, 2265 (1983)

31. R. S. Simon, M. V. Banaschik, R. M. Diamond, J. O. Newton, and F. S. Stephens, Nucl. Phys. A290, 253 (1977)

32. M. A. Deleplanque, H. J. Körner, H. Kluge, A. O. Macchiavelli, N. Bendjaballah, R. M. Diamond, and F. S. Stephens, Phys. Rev. Lett. 50, 409 (1983)

33. M. Jääskelainen, D. G. Sarantites, R. Woodward, F. A. Dilmanian, J. T. Hood, R. Jääskelainen, D. C. Hensley, M. L. Halbert, and J. H. Barker, Nucl. Instr. and Meth. 204, 385 (1983)

34. V. Metag, D. Habs, K. Helmer, U. v. Hemmolt, H. W. Heyng, B. Kolb, D. Pelte, D. Schwalm, W. Hennrich, H. J. Heinnrich, G. Himmele, E. Jaeschke, R. Repnow, W. Wahl, R. S. Simon, and R. Albrecht, Proc. of Geiger Memorial Meeting, Berlin, October, 1982

35. I. Y. Lee, Proceedings of Conference on High Angular Momentum Properties of Nuclei, Oak Ridge, TN, November, 1982. (Harwood Academic Publishers, New York, 1983) Ed. N. R. Johnson, p. 339

36. P. J. Twin, P. J. Nolan, R. Aryaeinejad, D. J. G. Love, A. H. Nelson, and A. Kirwan, Nucl. Phys. A409, 343c (1983)

37. R. M. Diamond and F. S. Stephens, The High Resolution Ball, unpublished, Sept., 1981

Fig. 1 A plot of angular momentum in a nucleus vs. the nuclear mass number. The curve ℓ_{II} traces out the points where the fission barrier is zero, according to the liquid-drop model. Below the curve ℓ_I the equilibrium shape is an oblate spheroid (Maclaurin); between ℓ_I and ℓ_{II} it is an ellipsoid, generally triaxial (Jacobi). The dashed line indicates a fission barrier of 8 MeV. (from ref. 10)

Fig. 2 The heavy lines constitute a phase-like diagram for the decay modes of a nucleus having mass number about 160 as a function of excitation energy and angular momentum. The lighter horizontal line indicates the range of angular momentum brought in by a typical heavy-ion reaction, following which two of the many possible decay pathways are shown (longer arrows represent neutron evaporations and shorter ones γ-ray emissions).

Fig. 3 This figure plots the ratio of the moment of inertia of a rigid ellipsoid to that of a rigid sphere as a function of the ellipsoidal shape parameter, γ. The two curves are for deformations ($\sim\Delta R/R$) of $\epsilon = 0.3$ and 0.6. The parameter γ defines a rotation axis, as well as a shape, and the four axially-symmetric shapes (two prolate and two oblate) are shown by the small drawings. The scale on the right converts the moment-of-inertia ratios into energy differences for a mass number around 160 and a spin of $60\hbar$. The dots indicate the energy differences from the full liquid-drop model (surface and Coulomb energies in addition to the rotational energy implied by the moment of inertia.)

Fig. 4 The level schemes are for the lowest-energy high-spin states in ^{158}Er and ^{147}Gd (Refs. 15, 16). The sketches on the left and right sides of the figure illustrate the dominant source of angular momentum in each case, collective rotation and single-particle alignment, respectively.

Fig. 5 Plots of the rotational period vs. time for the nucleus ^{158}Er (top) and the pulsar Vela (bottom).

Fig. 6 The two important coupling schemes in deformed nuclei. In the absence of rotation (top) particles with angular momentum, j, are in time-reversed orbits with projections $\pm\Omega$ along the symmetry (Z) axis. At high rotational frequencies the particles couple to a J, aligned as well as possible with the rotation (X) axis, along which they have projection, i.

Fig. 7 The aligned angular momentum, i, is plotted against rotational frequency, ω, for the first backbend ($i_{13/2}$ alignment) region of the lowest-lying (yrast) sequence in ^{162}Yb and of two bands in ^{163}Yb (labeled E and F). The midpoint of the sharp rise is approximately the crossing frequency (from Ref. 23).

Fig. 8 The shift in crossing frequency, $\delta\hbar\omega$, between the odd-neutron and neighboring even-even nucleus is plotted against the quadrupole moment of the odd-neutron orbit, $q_2(\nu)$. The configuration of the odd-neutron orbit is given by the Nilsson quantum numbers at the top. The dashed line illustrates the correlation between $\delta\hbar\omega$ and $q_2(\nu)$.

Fig. 9 A plot showing the correlations between two γ-ray energies following the reaction ^{124}Sn (^{40}Ar, xn) $^{164-x}Er$ at 185 MeV. The data were taken on Ge(Li) detectors and uncorrelated events were subtracted by the method of ref. 25. The plot shows contours of equal numbers of correlated events, according to the scale at the right (from ref. 27).

Fig. 10. The γ-ray spectrum (top) from the reaction indicated taken with a 5" x 6" NaI crystal and corrected for its response function. The spectrum corresponds to a rather broad distribution of initial spins centered around $55\hbar$ (ref. 24). The bottom plot is of $\mathcal{J}^{(2)}$ vs. $\hbar\omega$ as derived from the above data (heavy solid line). Also shown are similar plots for the systems $^{126}Te + ^{40}Ar$ (heavy dotted line) and $^{130}Te + ^{40}Ar$ (heavy dashed line) and some values for $\mathcal{J}^{(2)}$ for $^{124}Sn + ^{40}Ar$ (thin solid line) and $^{130}Te + ^{40}Ar$ (thin dashed line).

Fig. 11 A view of the Oak Ridge 4π NaI detector. There are 72 NaI detectors (each one attached to a protruding phototube and preamplifier) arranged in two hemispheres around the beam tube and (spherical) target chamber. One hemisphere is pulled back to allow access to the target chamber.

Fig. 12 Cutaway sketch of the detector system under construction at Berkeley (ref. 31). The inner "ball" consists of 44 bismuth-germanate (BGO) detectors arranged in three concentric cylinders, and will function much like the NaI ball in Fig. 11. (The photo tubes to be attached to the top or bottom of each element are not shown.) An array of 21 Compton-suppressed (BGO-shielded) germanium detectors surrounds the BGO ball and views the target through small holes in it. These detectors produce extremely high quality spectra in coincidence with events selected by the central ball.

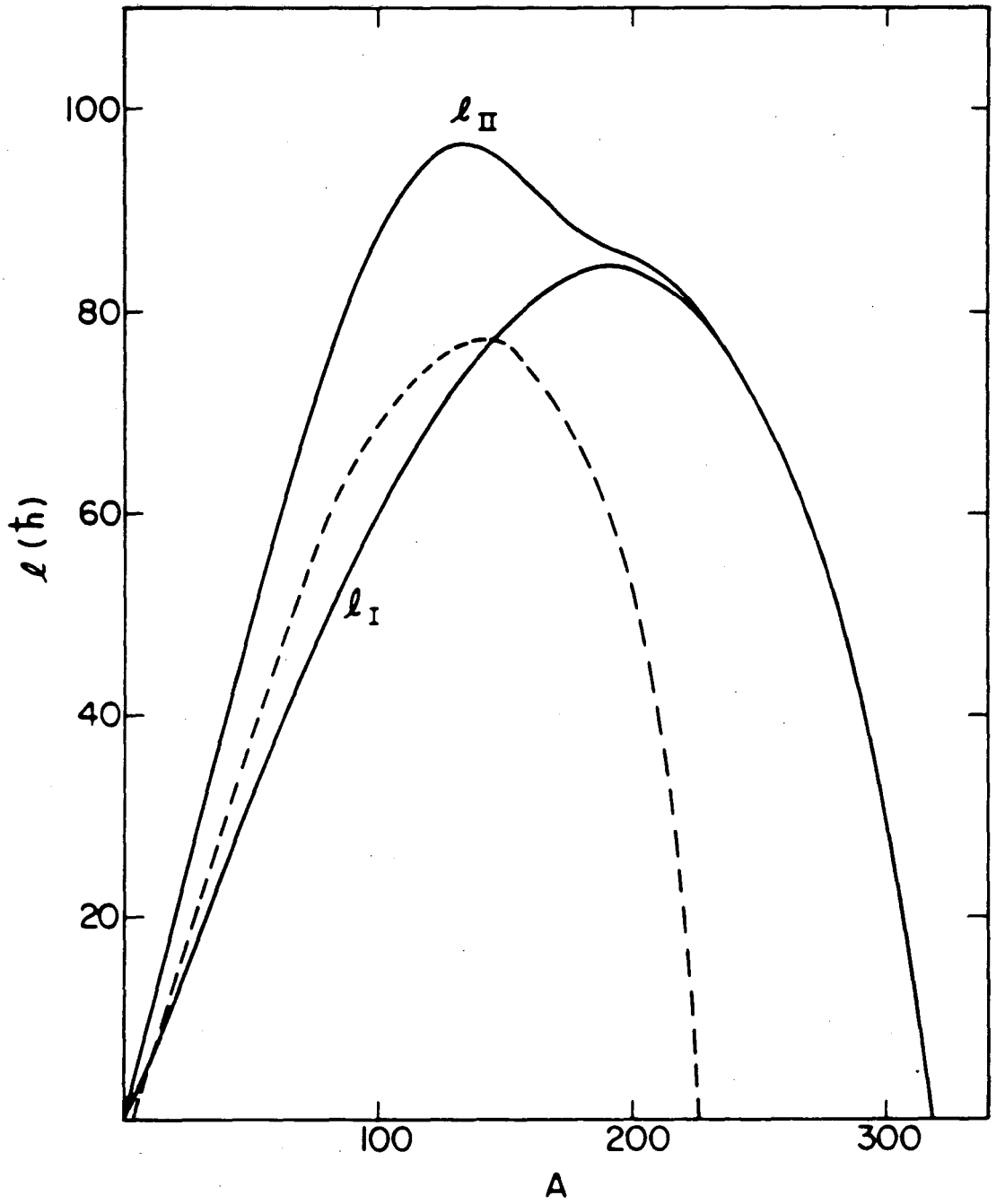

Fig. 1

XBL7210-4342

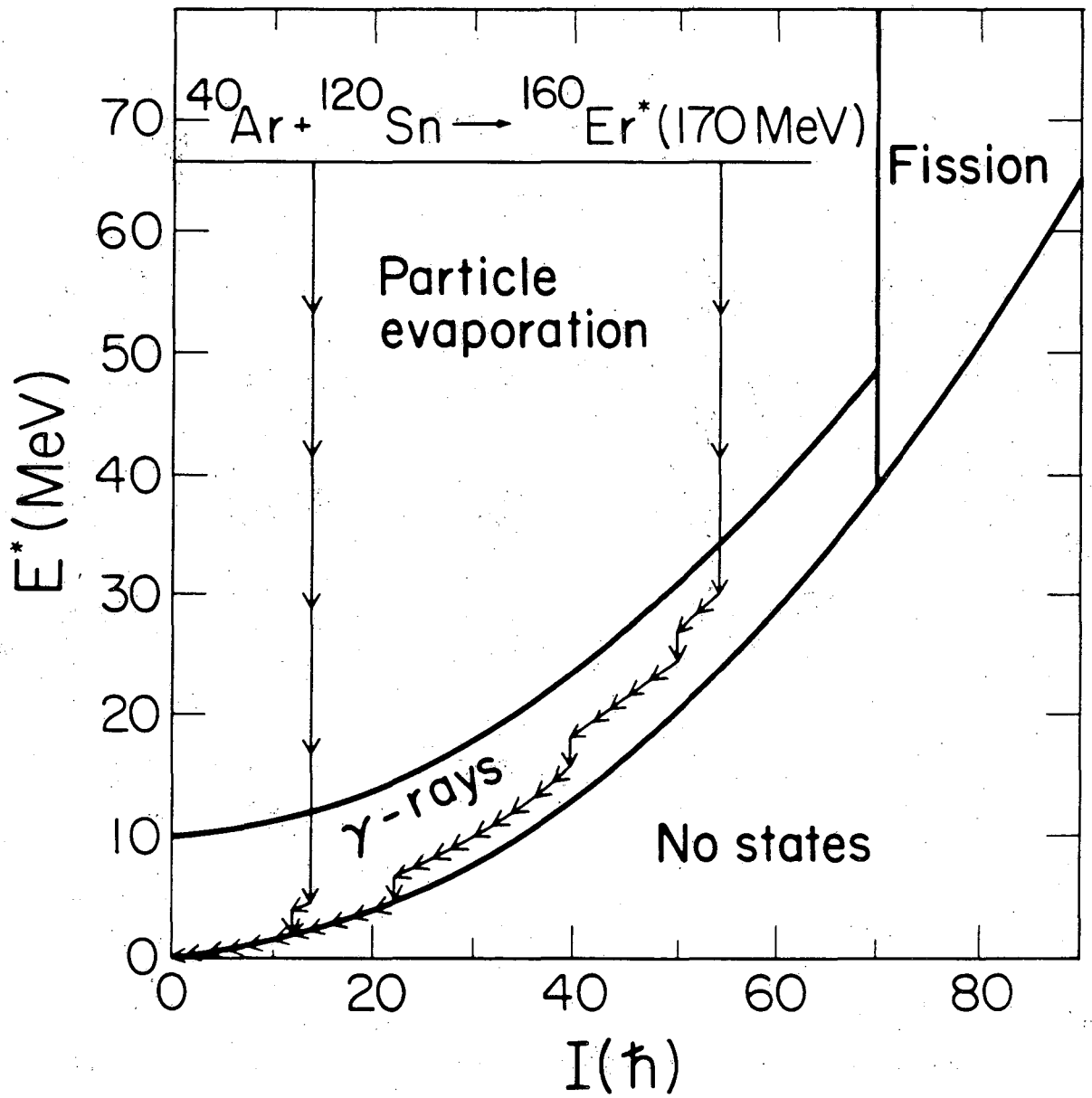

Fig. 2

XBL 833-1469

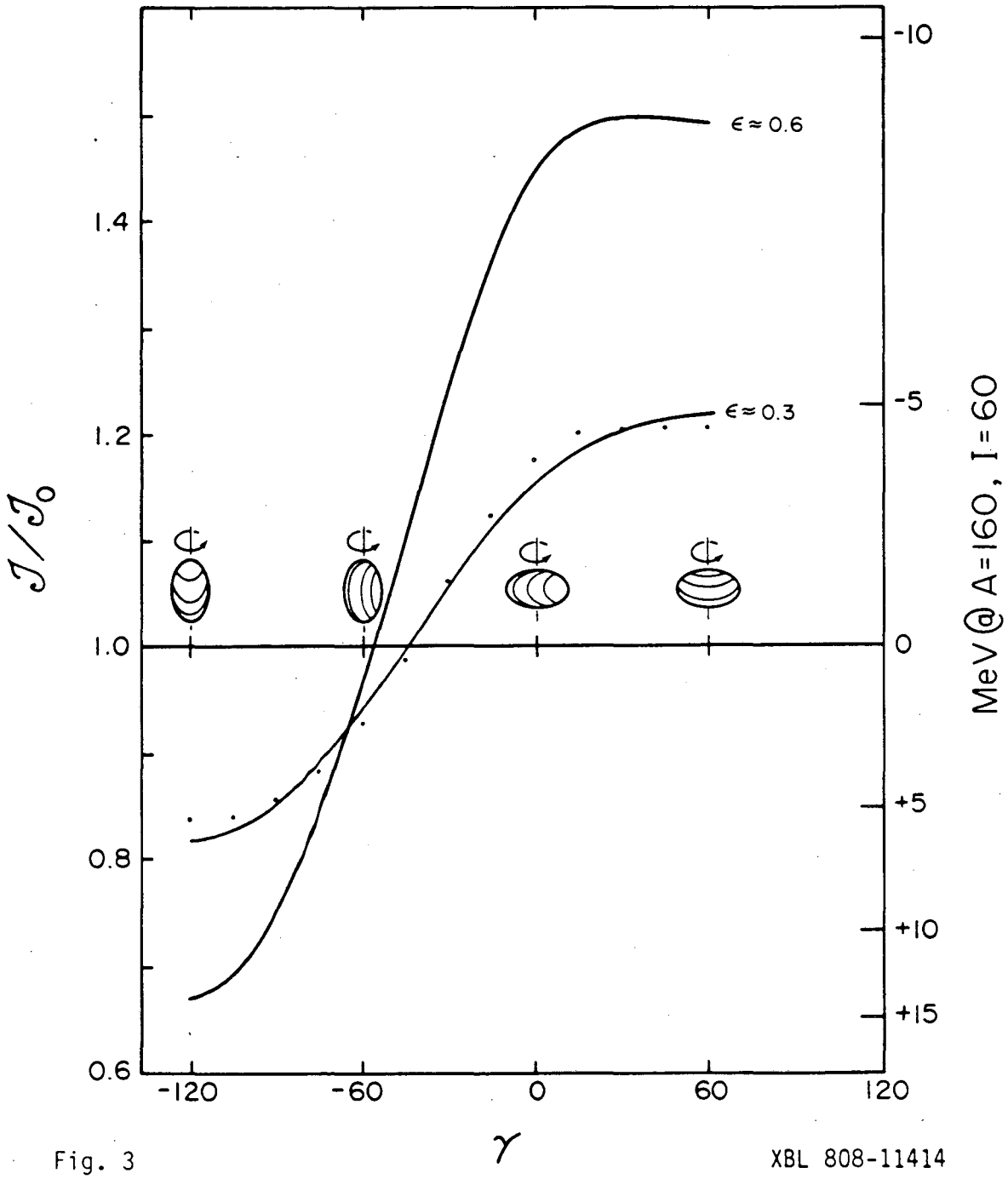

Fig. 3

XBL 808-11414

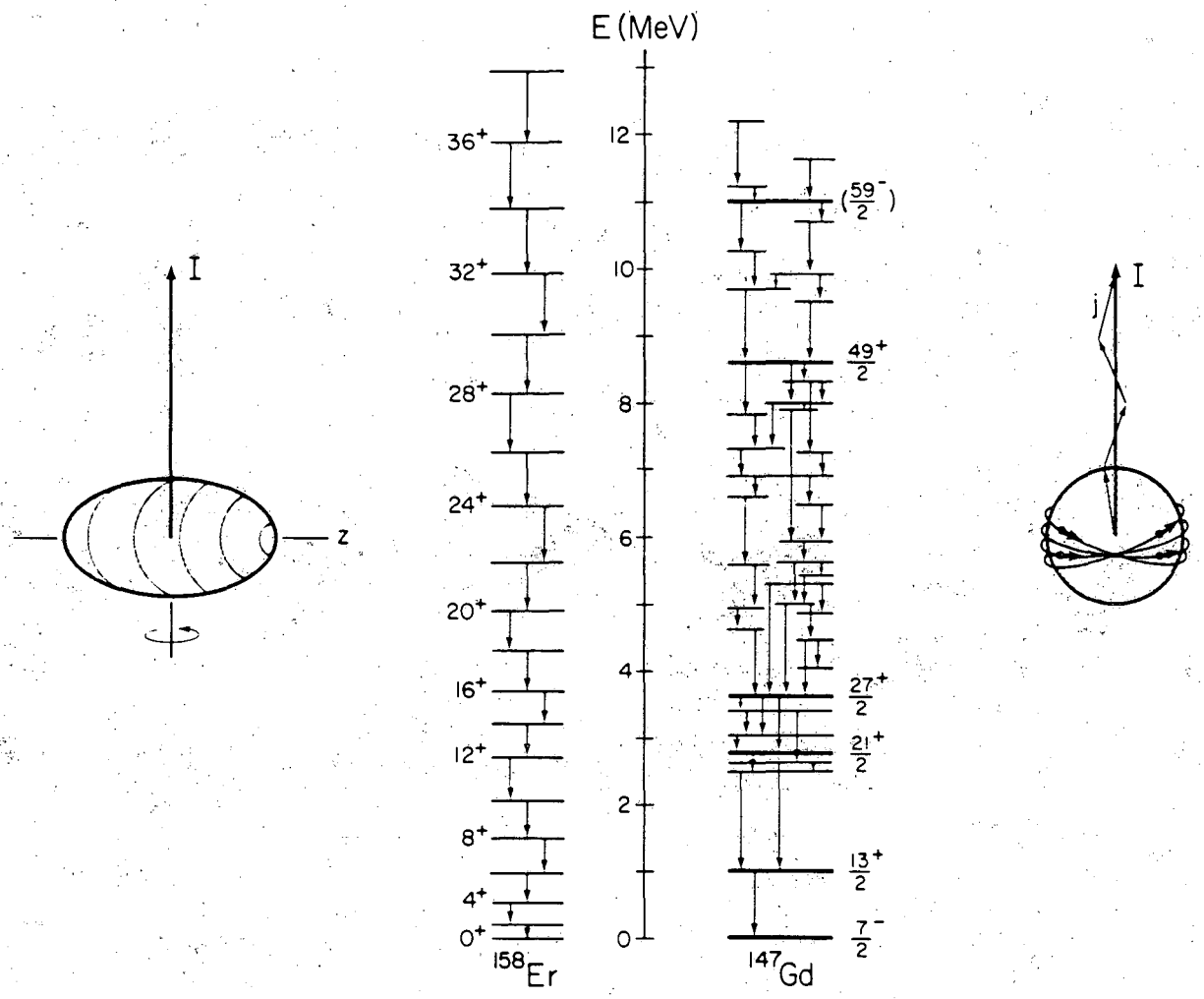

Fig. 4

XBL 828-1011

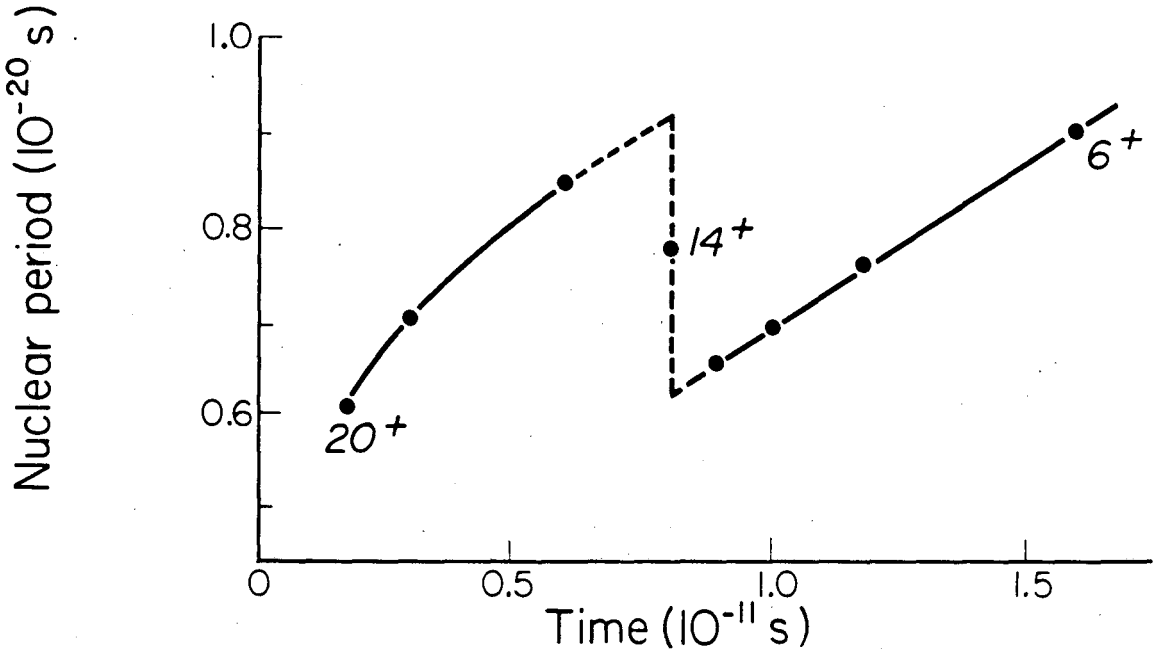

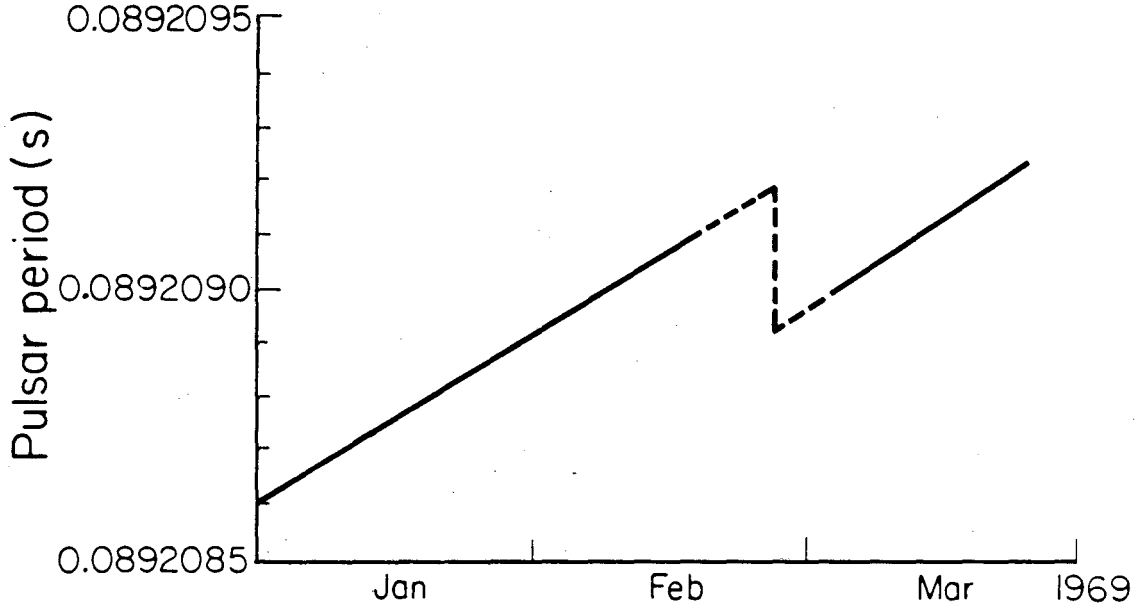

Fig. 5

XBL 826-10500

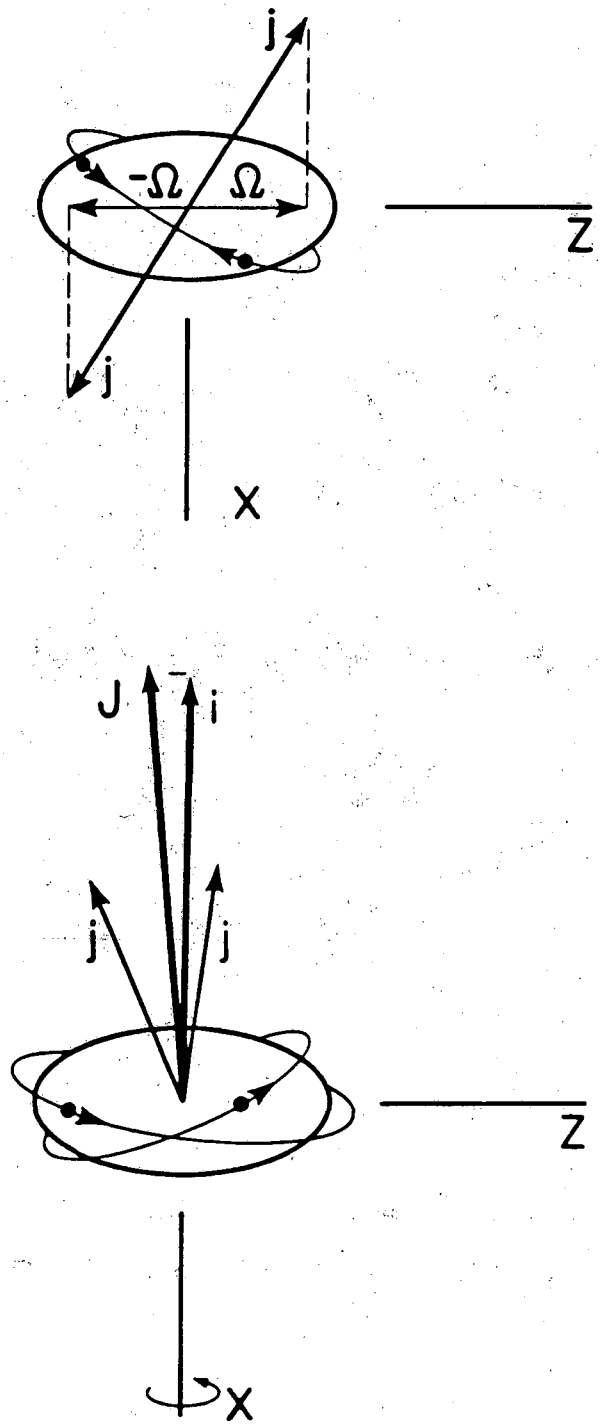

Fig. 6

XBL 833-1468

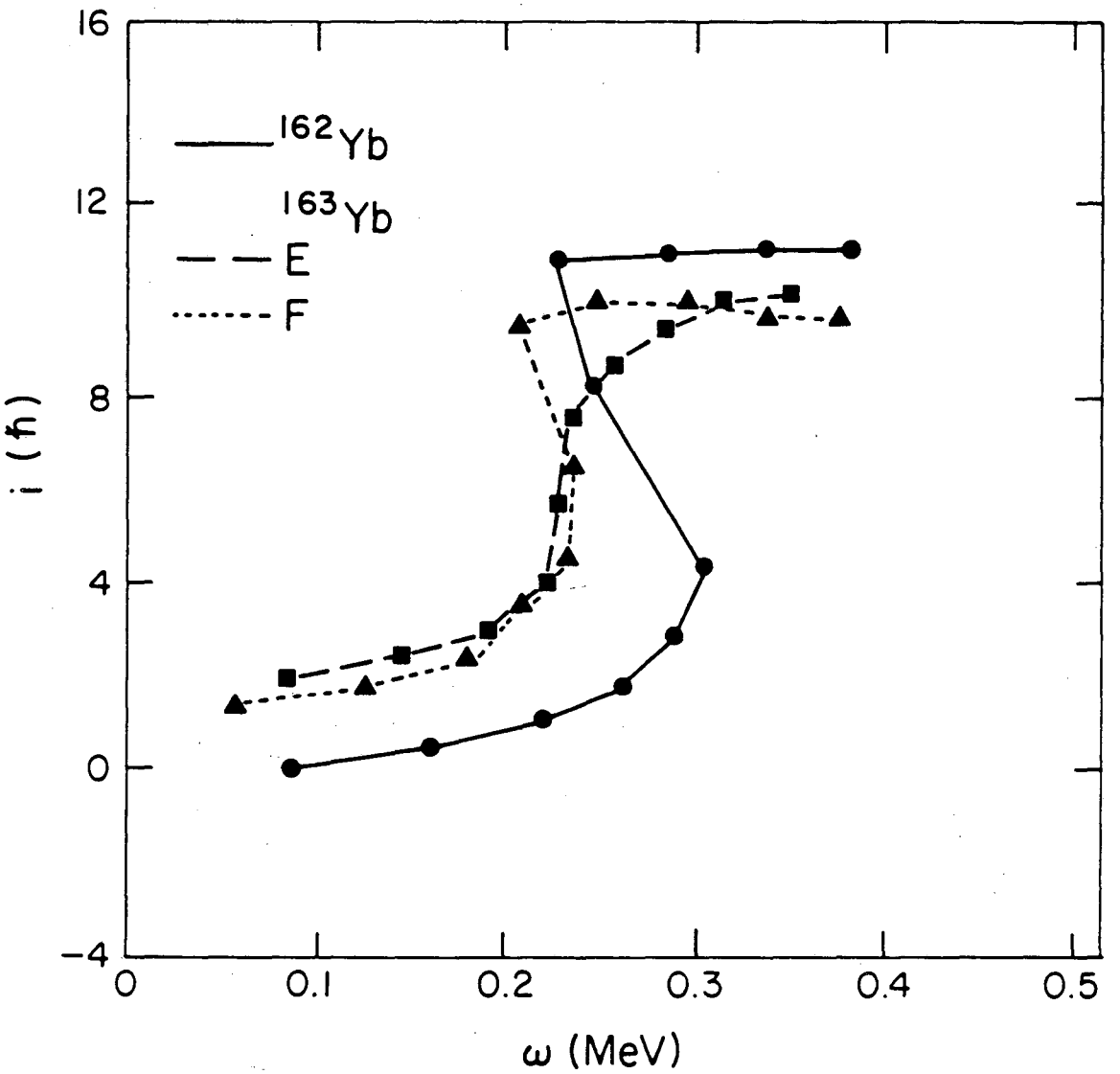

Fig. 7

XBL 828 – 1010

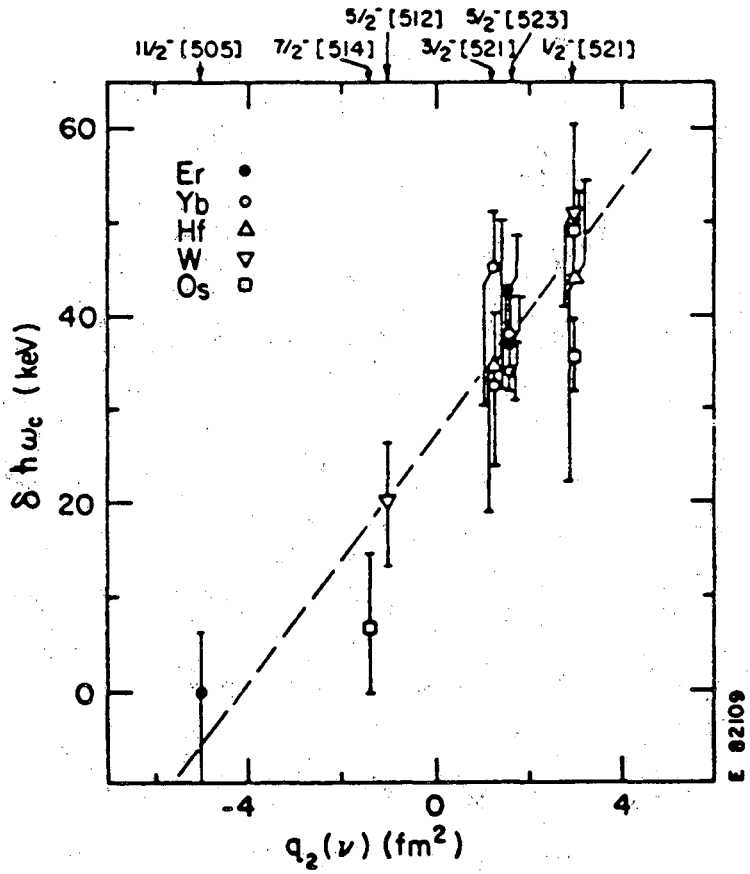

Fig. 8

XBL 834-9081

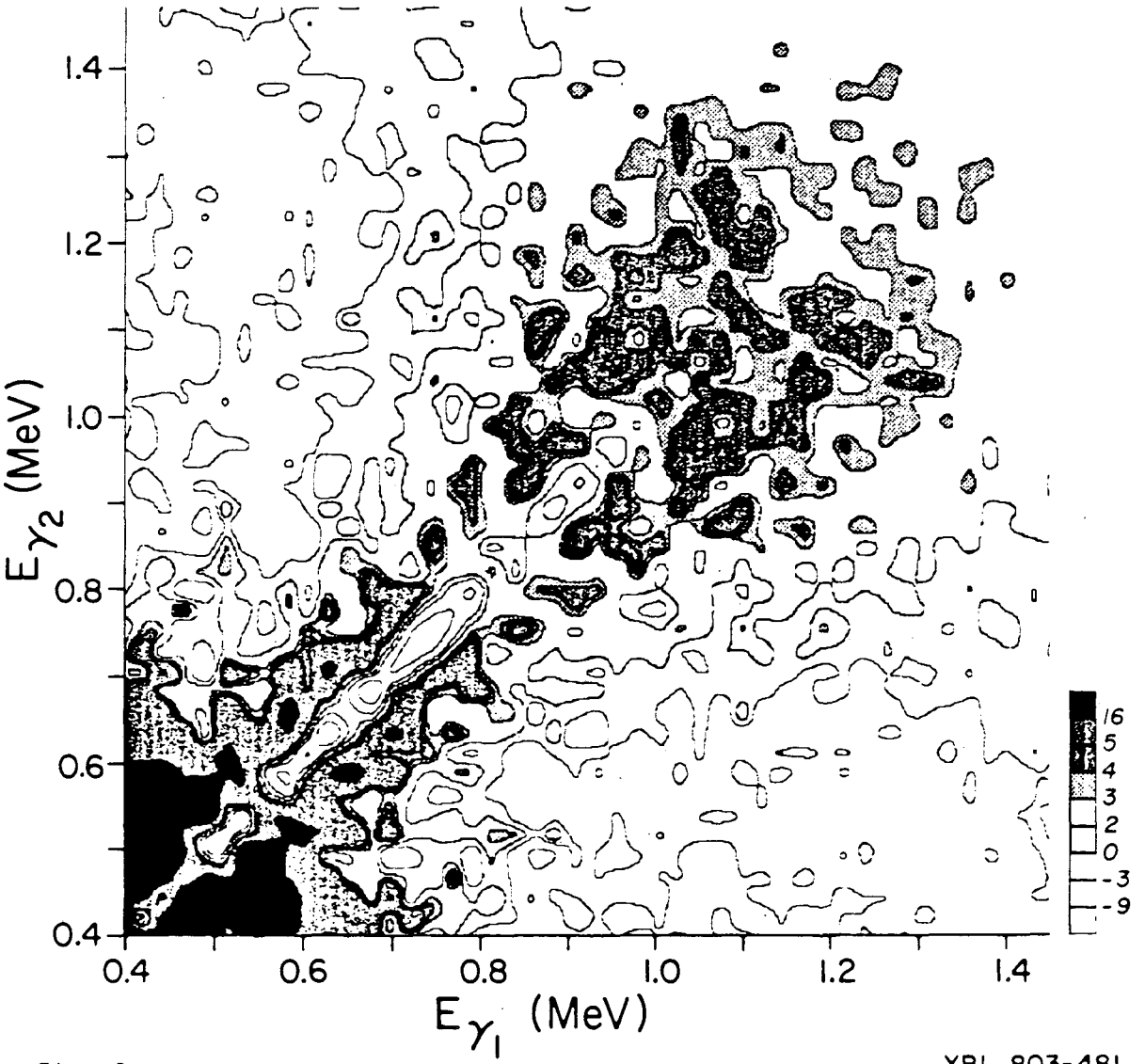

Fig. 9

XBL 803-481

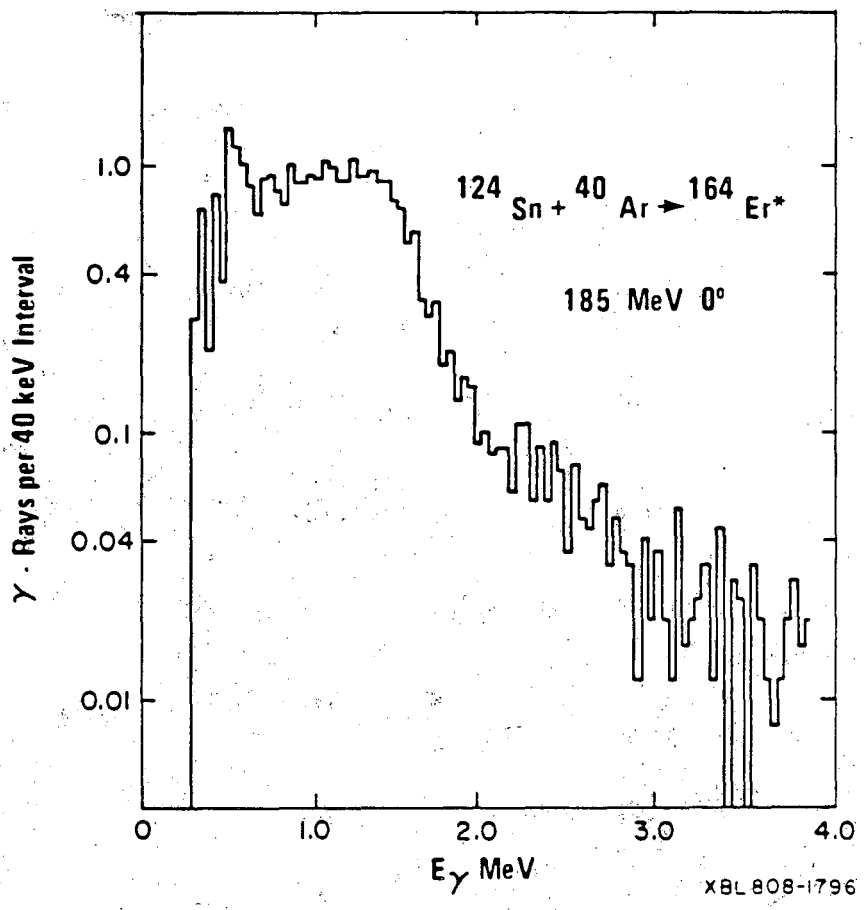
^{124}Sn + ^{40}Ar → ^{164}Er*
185 MeV 0°
γ · Rays per 40 keV Interval
1.0
0.4
0.1
0.04
0.01
0
1.0
2.0
3.0
4.0
E_γ MeV
XBL 808-1796

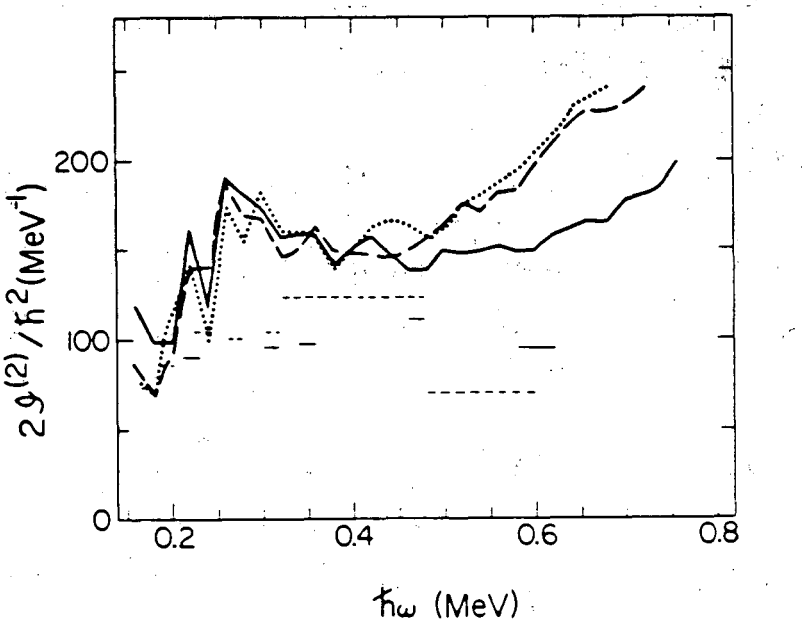
$2\mathcal{J}^{(2)}/\hbar^2$(MeV^{-1})
200
100
0
0.2
0.4
0.6
0.8
$\hbar\omega$ (MeV)

Fig. 10

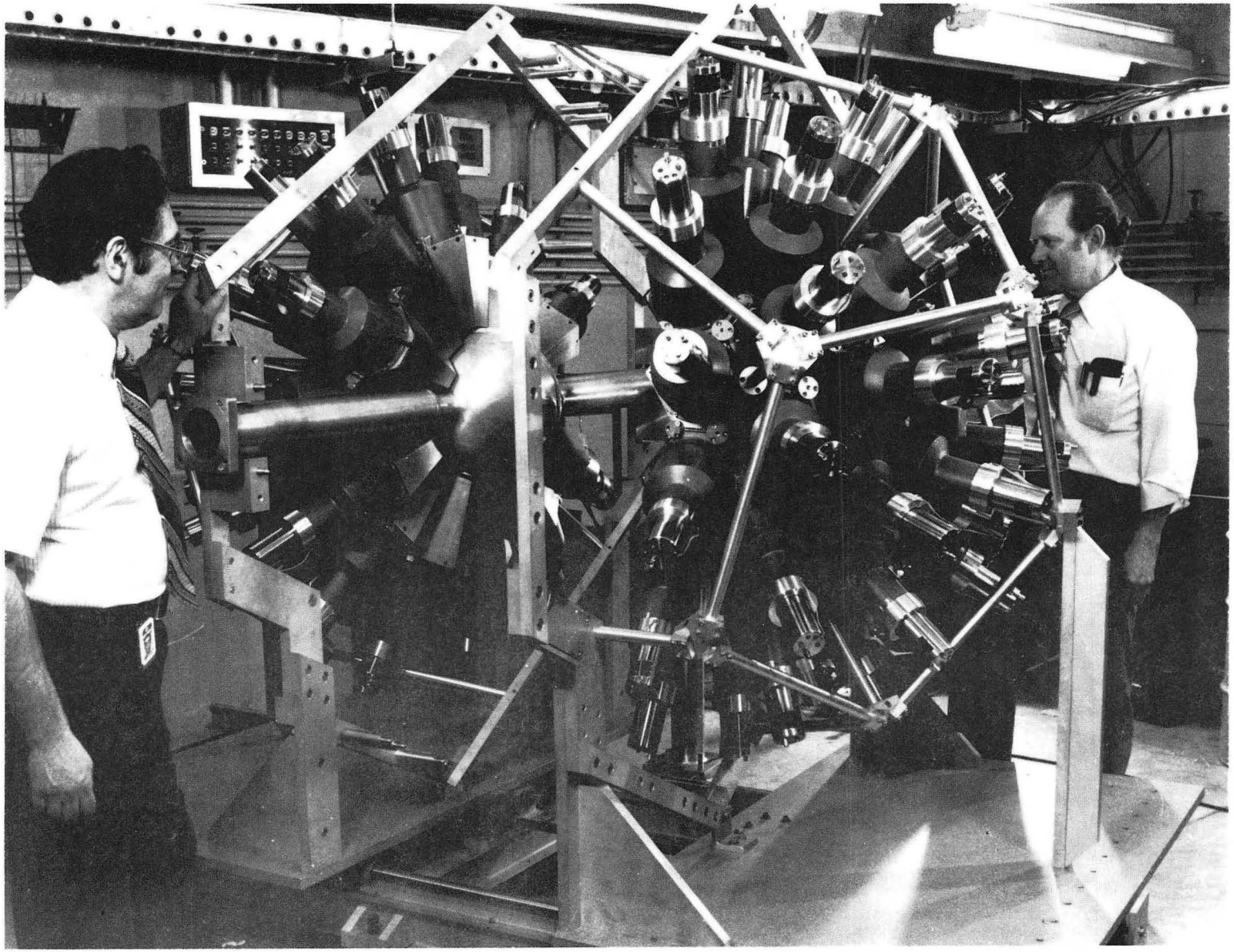

Fig. 11

XBB 809-10872

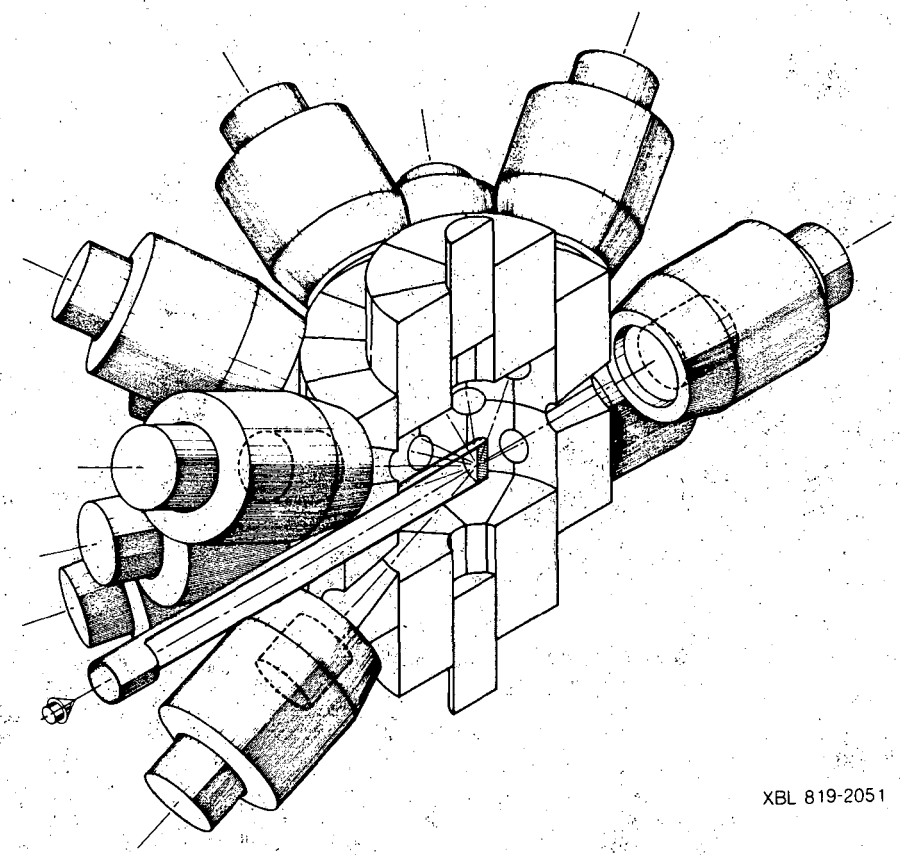

Fig. 12

This report was done with support from the Department of Energy. Any conclusions or opinions expressed in this report represent solely those of the author(s) and not necessarily those of The Regents of the University of California, the Lawrence Berkeley Laboratory or the Department of Energy.

Reference to a company or product name does not imply approval or recommendation of the product by the University of California or the U.S. Department of Energy to the exclusion of others that may be suitable.

TECHNICAL INFORMATION DEPARTMENT
LAWRENCE BERKELEY LABORATORY
UNIVERSITY OF CALIFORNIA
BERKELEY, CALIFORNIA 94720